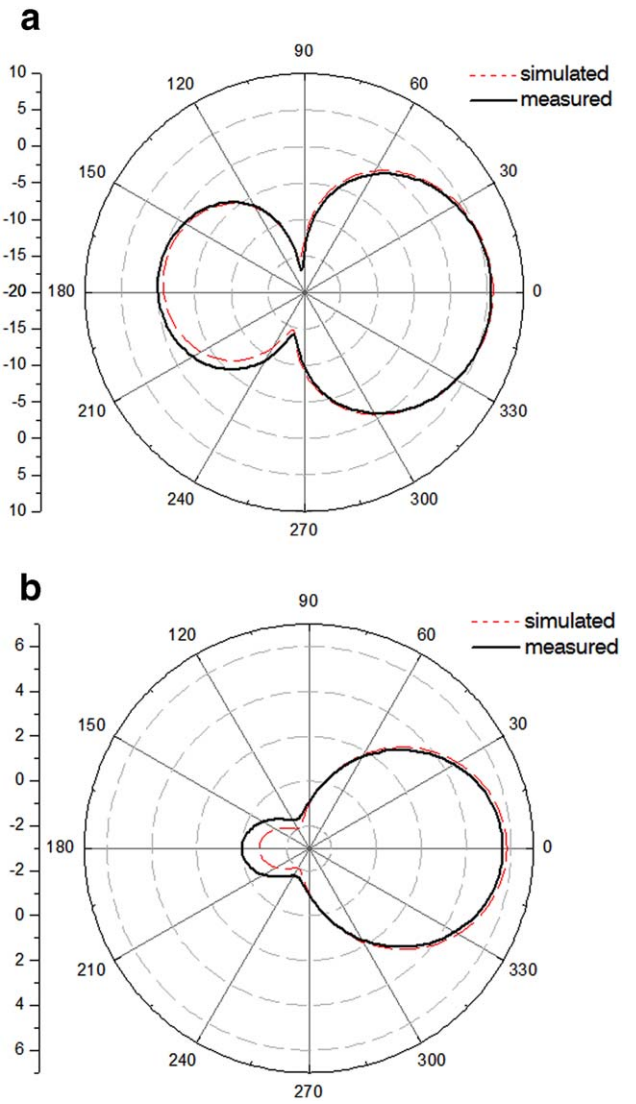

Figure 8 Simulated and measured radiation patterns of the proposed antenna at 5.2 GHz (a) E-Plane and (b) H-Plane. [Color figure can be viewed in the online issue, which is available at wileyonlinelibrary.com]

together with the simulation results in Figure 7. The simulated impedance bandwidth defined of 10 dB reaches 287 MHz (5.025∼5.312 GHz). For the measured result, the impedance bandwidth reaches over 242 MHz (5.145∼5.387 GHz), which covers the 5.2 GHz WLAN frequency band. The measured result has slight discrepancy with the simulation due to the limitation of SMA connector and its mechanical tolerance, which have been neglected in our simulations.

The far-field radiation pattern of the proposed antenna in the E-plane and H-plane at 5.2 GHz is shown in Figure 8. From Figure 8(a), one can see that the corresponding maximum gain and half-power beam width (HPBW) are 5.8 dBi and 81.3° in the E-plane, respectively. In the Figure 8(b), it can be noted that in the H-plane there exists the maximum gain and HPBW are 5.8 dBi and 101.4°, respectively. The operating bandwidth of the proposed antenna with usable broadside radiation patterns was found to be about 242 MHz (5.145∼5.387 GHz), which is consistent with the specification of the WLAN system. The obtained results show a qualitative agreement between the simulation and the measurements data.

4. CONCLUSION

A simple printed of WLAN antenna has been designed, fabricated, and measured. The antenna has an M-shaped patch radiator on one side of the substrate and spiral CSRR shape on the other side. Simulated and measured results are presented to validate the usefulness of this small proposed antenna structure for WLAN applications. The antenna dimension is 25 × 25 × 0.8 mm^3. The proposed antenna has stable radiation patterns, small size and relative high gains. So, the presented antenna is a good choice to WLAN communication systems.

ACKNOWLEDGMENTS

This work was supported by the National Natural Science Foundation of China (no. 60971027 and no. 61131005) and by the Zhejiang Province Natural Science Fund for Distinguished Young Scientists (LR12F05001). The authors would like to express their sincere appreciation to these supports.

REFERENCES

1. Y.C. Lin and K.J. Hung, Compact ultra-wideband rectangular aperture antenna and band-notched designs, IEEE Trans Antennas Propag 54 (2006), 3075–3081.
2. S.L. Latif, L. Shafai, and S.K. Shaema, Bandwidth enhancement and size reduction of microstrip slot antenna, IEEE Trans Antennas Propag 53 (2005), 994–1003.
3. S.Q. Xiao, B.Z. Wang, W. Shao, and Y. Zhang, Bandwidth enhancing ultra low profile compact patch antenna, IEEE Trans Antennas Propag 53 (2005), 3443–3447.
4. Y. Luo, Y.Z. Ying, and Y.Y. Guo, A dual-wideband antenna with an open L-slot for WLAN/Wimax applications, Microwave Opt Technol Lett 54 (2012), 1499–1502.
5. J.Y. Sze and K.L. Wong, Slotted microstrip antenna for bandwidth enhancement, IEEE Trans Antennas Propag 48 (2005), 1149–1152.

THE DESIGN OF DOUBLE RIDGE WAVEGUIDE FILTER USING CONVENTIONAL STEPPED IMPEDANCE LOW-PASS FILTER METHOD

Mohsen Yazdani,[1] Luke Murphy,[1] Alireza Mallahzadeh,[2] Ercument Arvas,[1] and Joseph Mautz[1]

[1] Syracuse University, Syracuse, NY, 13214, USA; Corresponding author: mvazdani@svr.edu

[2] Shahed University, Tehran, Iran

Received 20 May 2013

ABSTRACT: A *simple design procedure for a double ridge waveguide low-pass filter (LPF) is proposed in this article. The procedure follows similar steps involved in a stepped impedance microstrip LPF. The starting point is calculating lumped element low-pass prototypes and converting them to the double ridge waveguide sections. Step discontinuities are also studied and a lumped element model is proposed by comparing S parameters calculated by HFSS software. The results are then applied to design a six order maximally flat double ridge LPF with 4 GHz cutoff frequency.* © 2014 Wiley Periodicals, Inc. Microwave Opt Technol Lett 56:120–124, 2014; View this article online at wileyonlinelibrary.com. DOI 10.1002/mop.28022

Key words: *double ridge waveguide; low-pass filter; stepped impedance filter; step discontinuity*

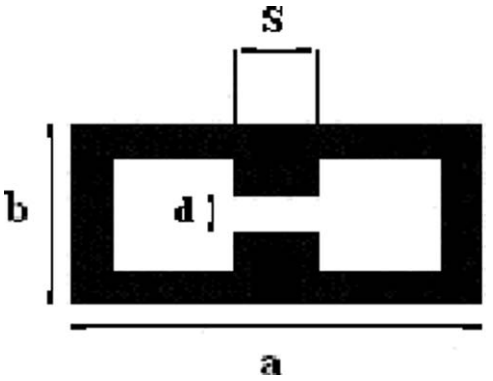

Figure 1 Cross section of the double ridge waveguide

1. INTRODUCTION

Microwave low-pass filters (LPFs) are used widely in satellite communications and other microwave telecommunication systems [1]. One of the most commonly used LPFs topologies is stepped impedance LPF designed by microstrip or coaxial lines [2]. Fixed impedance over wide frequency range and design ease of low and high impedance elements, make microstrip and coaxial lines the most commonly used transmission line systems when designing low power stepped impedance LPFs.

On the other hand, double ridge waveguide of Figure 1, is well known for a lower cutoff frequency at dominant mode with respect to the conventional waveguide, wider bandwidth free from higher-order modes, low characteristic impedance, and almost fixed impedance characteristic over a large frequency range [3,4]. Therefore, these features make it a potential candidate for design of high power stepped impedance LPF.

In recent years, many works have been done on design of low-pass double ridge waveguide filters. In [5,6], a double ridge waveguide LPF implemented by S-matrix method is introduced. Mode matching technique is also applied to the design of E-plane ridge waveguide filters [7]. However, none of above methods have proposed a simple topology on designing double ridge waveguide filters.

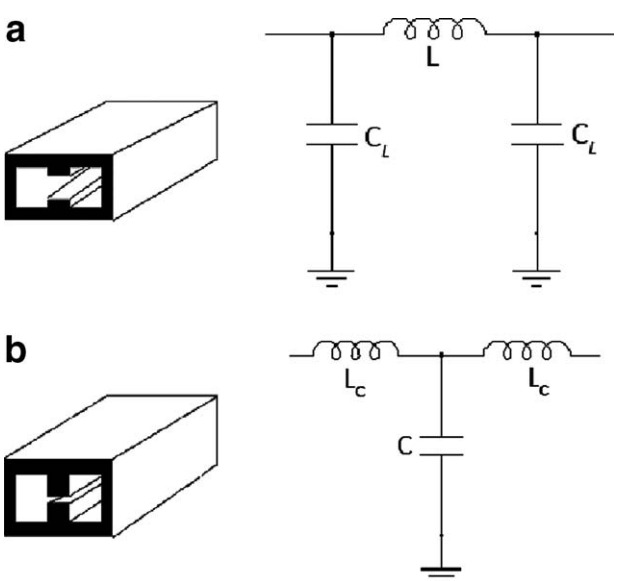

Figure 2 (a) High-impedance double ridge waveguide section and equivalent circuit model and (b) Low-impedance double ridge waveguide section and equivalent circuit model

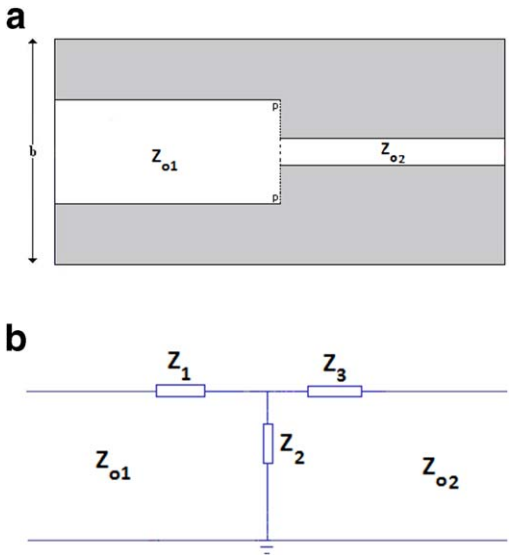

Figure 3 (a) Double ridge step discontinuity and (b) equivalent circuit model. [Color figure can be viewed in the online issue, which is available at wileyonlinelibrary.com]

A design procedure for a double ridge waveguide LPF using a stepped impedance concept is proposed in this article. A six order maximally flat double ridge waveguide LPF with 4 GHz cutoff frequency is designed and fabricated by this method.

The simulation of the proposed filter has been carried out using HFSS software and its various characteristics have been thoroughly investigated.

2. DESIGN AND IMPLEMENTATION PROCEDURE

2.1. Design Procedure

The design of the stepped impedance low pass double ridge waveguide filter involves two main steps. The first step is to select an appropriate low-pass prototype based on desired response characteristics.

The element values of the low-pass prototype filter are then transformed to the L-C elements for the desired cutoff frequency and source impedance.

In the design procedure of stepped impedance LPFs [2], low and high impedance transmission lines will be modeled with T

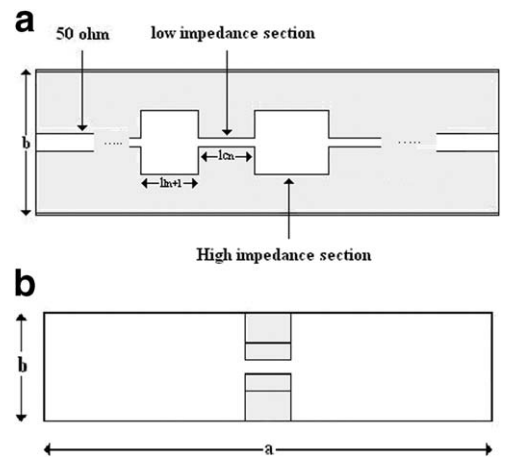

Figure 4 The proposed filter structure (a) longitudinal section and (b) cross section

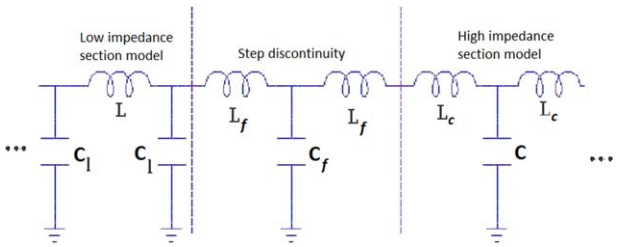

Figure 5 Equivalent circuit model of the proposed filter. [Color figure can be viewed in the online issue, which is available at wileyonlinelibrary.com]

and Π circuits shown in Figure 2, where L and C are prototypeinductor and capacitor values. Shunt capacitor C_l and series inductor L_c are calculated by:

$$c_l = \frac{\tan\left(\pi l_l/\lambda_g\right)}{Z_{0l}\omega} \tag{1}$$

$$l_c = \frac{z_{0c}\tan\left(\pi l_c/\lambda_g\right)}{\omega}. \tag{2}$$

The second step involves designing appropriate double ridged waveguide sections to approximate L and C elements.

To calculate C_l and l_c in Eqs. (1) and (2), one could find the impedance of double ridge waveguide by [8]:

$$z_{oi} = \frac{\pi\eta_o\left(\frac{b}{a}\right)\left(\frac{d_i}{b}\right)\left(\frac{a}{\lambda_{ci}}\right)}{\left[\left(\frac{b}{a}\right)\left(\frac{d_i}{b}\right)\left(\frac{2a}{\lambda_{ci}}\right)\ln\cos ec\left(\frac{\pi d_i}{2b}\right)\cos^2\theta_2+\frac{\theta_2}{2}+\sin\frac{2\theta_2}{4}\right.}$$
$$\left.+\left(\frac{d_i}{b}\right)\left(\frac{\cos(\theta_2)}{\sin(\theta_1)}\right)^2\left[\frac{\theta_1}{2}-\sin\frac{2\theta_1}{4}\right]\right]$$
$$\theta_1=\pi\left(1-\frac{s}{a}\right)\frac{a}{\lambda_c}\theta_2=\pi\left(\frac{s}{a}\right)\frac{a}{\lambda_c} \tag{3}$$

where wavelength may be found using:

$$\frac{b}{\lambda_{cr_i}}=\frac{b}{2(a-s)}$$

$$\left[1+\frac{4}{\pi}\left(1+0.2\sqrt{\frac{b}{(a-s)}}\right)\left(\frac{b}{(a-s)}\right)\ln\cos ec\left(\frac{\pi d_i}{2b}\right)\right.$$
$$\left.+\left(2.45+0.2\frac{s}{a}\right)\left(\frac{sb}{d_i(a-s)}\right)\right]^{-\frac{1}{2}} \tag{4}$$

- $i=l$ or H

$$\frac{\lambda_g}{\lambda_c}=\left[1-\left(\frac{\lambda_c}{\lambda_{cr}}\right)^2\right]^{-\frac{1}{2}}$$

where λ_g, λ_{cr}, and λ_c are guide wavelength of double ridge, cutoff wavelength of double ridge waveguide and cutoff wavelength of filter, respectively. The step discontinuity between two double ridge waveguide sections can be modeled by an equivalent T circuit illustrated in Figure 3. The S parameters of the step discontinuity are calculated by HFSS and compared with the S matrix parameters of the equivalent model. The results show that the equivalent parallel and series elements can be modeled by a capacitor and inductors, respectively.

TABLE 1 Six Order Maximally Flat LPF Prototype Values

g_0	g_1	g_2	g_3	g_4	g_5	g_6	g_7
1	0.5176	1.414	1.932	1.932	1.414	0.5176	1

TABLE 2 Gapacitance and Inductance Values in Cutoff Frequency

C_1 (pF)	C_3 (pF)	C_5 (pF)	L_2 (nH)	L_4 (nH)	L_6 (nH)
0.41189	1.5374	1.1252	2.8131	3.8436	1.0297

TABLE 3 The Characteristic Impedances of the Proposed Filter

Characteristic Impedance	Z_{0L}	Z_0	Z_{0H}
Impedance Amplitude (Ω)	12	50	102
Double Ridge Gap (mm)	0.2	1.2	4.6

TABLE 4 Capacitance and Inductance Values of Ridge Discontinuities

Parameters of Step Discontinuity	Z_0-Z_{0H}	$Z_{0H}-Z_{0L}$	$Z_{0H}-Z_0$
C_f (pF)	0.048	0.157	0.104
L_f (Nh)	0.072	0.998	0.546

The physical lengths of the high and low impedance sections may be found by the formula given below:

$$l_l=\lambda g/2\pi\sin^{-1}(\omega_c L\ /\ Z_l) \tag{5}$$

$$l_c=\lambda_g/2\pi\sin^{-1}(\omega_c\ C\ Z_c) \tag{6}$$

where L and C are final values or inductance and capacitance calculated by an iteration technique.

Figure 4 depicts cross and longitudinal sections of the proposed double ridge waveguide LPF and the equivalent lumped element circuit is shown in Figure 5.

2.2. Design Example and Implementation Procedure

The specifications for the filter under consideration are Cutoff frequency $f_c = 4$ GHz and Source/load impedance $z_0 = 50$ Ω. A

TABLE 5 The Final Length of the Ridge Sections

l_{c1}(mm)	l_{l2} (mm)	l_{c3} (mm)	l_{l4} (mm)	l_{c5} (mm)	l_{l6} (mm)
1	4	4	5.25	4.5	1

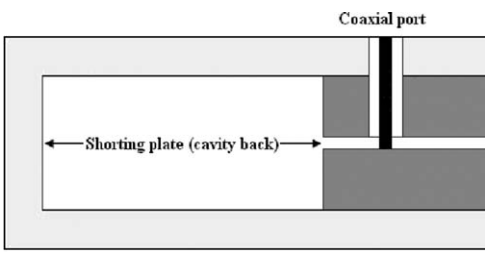

Figure 6 Double ridge to coaxial cable transition

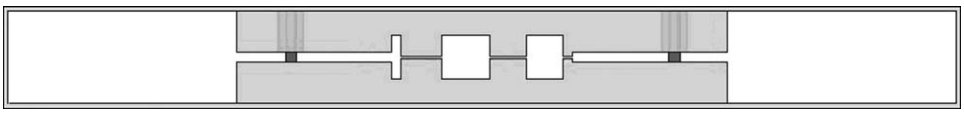

Figure 7 Longitudinal section of the proposed filter

Figure 8 Fabricated double ridge LPF filter. [Color figure can be viewed in the online issue, which is available at wileyonlinelibrary.com]

six order maximally flat LPF prototype is chosen and transferred to the desired frequency. The prototype element values and capacitance/inductance values are shownin Tables 1 and 2, respectively.

Therefore, by choosing the characteristic impedances of the low-Z, $z0_L$, and high-Z sections, Z_{0H} Table 3, and calculating the parameters of the step discontinuities, Table 4, the final length of the sections, Table 5, can be calculated by (5) and (6).

It is necessary to use an appropriate transition between coaxial probes and 50 Ω double ridge waveguide at input and output ports. Entrance of the coaxial probes is critical for the return loss performance of the filter.

Many simulations have been made to optimize the transitional performance of coaxial cable to double ridge waveguide using Ansoft HFSS. For good return loss, two features are necessary:

a. The inner conductor of the coaxial probes passes through the first ridge and is then connected to the opposite ridge, Figure 6.
b. A shorting plate (cavity back) is used to obtain good return loss in double ridge waveguide transition, Figure 6. The distance from the double ridge waveguide ends to the shorting plate is selected to be 1.5 cm.

Figures 7 and 8 show the longitudinal section and the fabricated filter, respectively.

Figure 9 shows a comparison between simulation results of proposed filter and the conventional lumped element LPF. The simulated results are in good agreement with conventional ones.

3. MEASUREMENT

Measurements were carried out using an Agilent Network Analyser hp-8410C. As shown in Figure 10, the performance of the fabricated filter is acceptable. The proposed filter has a good stop-band performance at 4–10 GHz and insertion loss less than 0.6 dB in the pass-band area. A good agreement between experimental and simulated results is obtained.

4. CONCLUSION

A design procedure for a stepped impedance double ridge waveguide LPF is presented in this article. The S parameters of double ridge step discontinuities are calculated by HFSS and compared with those of proposed equivalent circuit model. It has been shown that all types of lumped element LPFs can be obtained as double ridge waveguide LPFs. A six order maximally flat double ridge waveguide LPF with 4 GHz cutoff frequency is then designed and fabricated by this method.

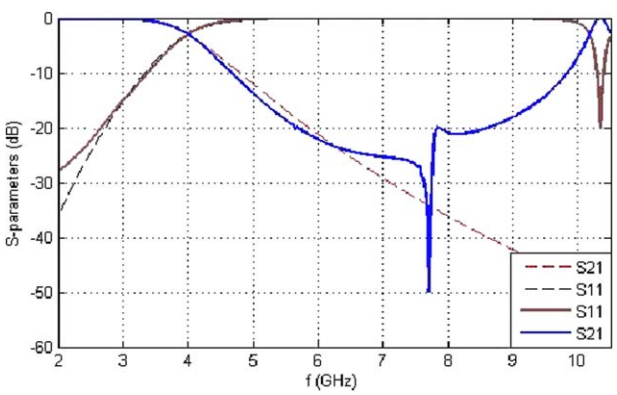

Figure 9 Comparison between simulation results of the double ridge maximally flat LPF and the conventional maximally flat filter. [Color figure can be viewed in the online issue, which is available at wileyonlinelibrary.com]

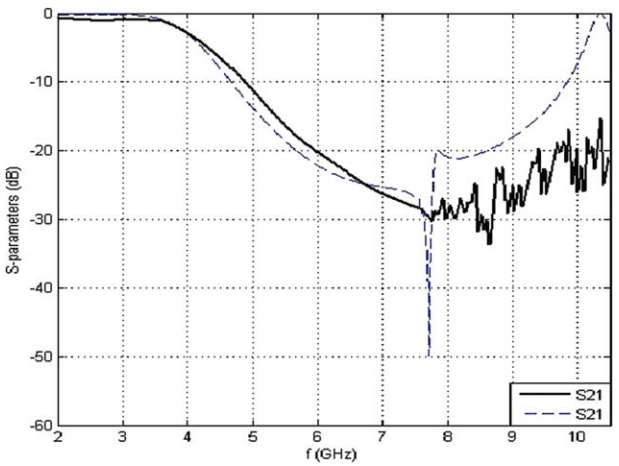

Figure 10 Comparison between simulation results of the double ridge maximally flat LPF and the conventional lumped element maximally flat filter. [Color figure can be viewed in the online issue, which is available at wileyonlinelibrary.com]

REFERENCES

1. W. Hauth, R. Keller, and U. Rosenberg, CAD of waveguide low-pass filters for satellite applications, In: 17th European Microwave Conference, Rome, 1987, pp. 151–156.
2. G.L. Matthaei, L. Young, and E.M.T. Jones, Microwave filters, impedance matching networks and coupling structures, McGraw Hill, New York, NY, 1980.
3. J. Helszajn, Ridge waveguides and passive microwave components, The Institute of Electrical Engineers, London, 2000.
4. S.B. Cohn, Properties of ridge waveguide, Proc IRE 35 (1947), 783–788.
5. S. Li, J. Fu, and X. Wu, Double ridged waveguide low pass filters for satellite application, In: International Symposium on Microwave, Antenna, Propagation, and EMC Technologies for Wireless Communications, August 2007, pp. 408–410.
6. J. Bornemann and F. Arndt, Modal S-matrix design of metal finned waveguide components and its application to transformers and filters, IEEE Trans Microwave Theory Tech 40 (1992), 1528–1537.
7. A.M.K. Saad, Novel low-pass harmonic filters for satellite application, In IEEE MTT-S International Microwave Symposium Digest, San Francisco, CA, 1984, pp. 292–294.
8. S. Hopfer, The design of ridged waveguide, IRE Trans Microwave Theory Tech 5 (1955), 20–29.
9. A.M.K. Saad, J.D. Miller, A. Mitha, and R. Brown, Analysis of antipo-dal ridge waveguide structure and application on extremely wide stopband lowpass filter, In: Proceedings of 1986 IEEE MTT-S International Microwave Symposium Digest, Baltimore, MD, 1986, pp. 361–363.

A STUDY OF TRANSMISSION OF RF SIGNAL WITH SINGLE CONDUCTOR WIRE

Zicong Mei,[1] Sai Ho Yeung,[1] Tapan K. Sarkar,[1] and Magdalena Salazar-Palma[2]

[1] Department of Electrical Engineering and Computer Science, Syracuse University, Syracuse, NY 13244-1240; Corresponding author: zmei@syr.edu

[2] Departmento de Teoria de la Senal y Communicaciones, Universidad Carlos III de Madrid, 28911 Leganes, Madrid, Spain

Received 1 May 2013

ABSTRACT: *Some researches showed that a single conductor wire can transmit signals. We tried to duplicate these results and we can see a single conductor wire does transmit signals. But its performance is very poor, especially when the wire is not a straight wire.* © 2014 Wiley Periodicals, Inc. Microwave Opt Technol Lett 56:124–127, 2014; View this article online at wileyonlinelibrary.com. DOI 10.1002/mop.28058

Key words: *sommerfeld; single conductor wire; propagation*

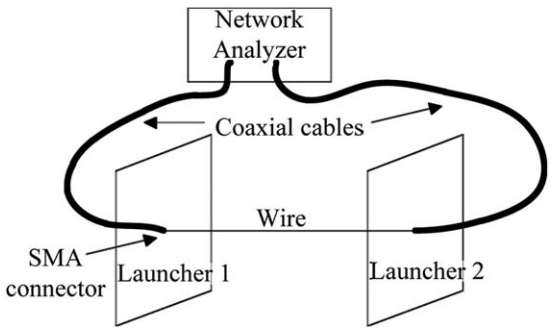

Figure 1 The experiment setup

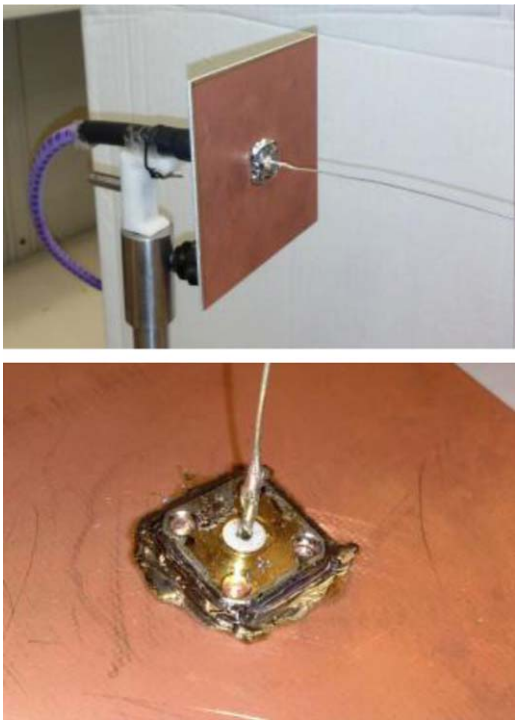

Figure 2 The launcher. [Color figure can be viewed in the online issue, which is available at wileyonlinelibrary.com]

1. INTRODUCTION

A nonradiating wave along a conducting cylinder was derived by Sommerfeld. [1–4] Many researchers tried to apply it to transmit signals along a single conducting wire. Many of such kind researches focused on terahertz frequencies. [5–8] But there are some researchers applied it to a lower frequency. [4,9,10]

In [4], the Sommerfeld wave is analyzed analytically to obtain the propagation constant and attenuation. Theoretical analysis shows that the attenuation for waves around GHz is not very large. For example, the surface wave on a copper wire with 1-mm radius has an attenuation of 0.4 dB per 100 ft. at 1 GHz. [4] Thus, it is possible to use a single conductor wire to transmit signals.

In [10], it is showed that besides TEM wave, a TM surface wave also exists in coaxial cable. When the size of the outer conductor

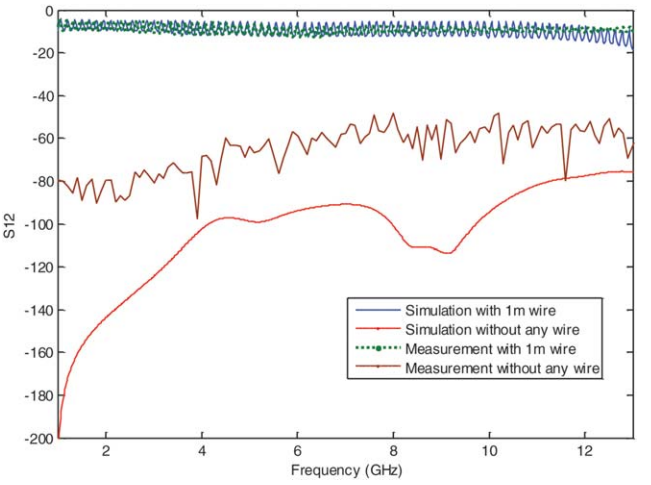

Figure 3 The comparison of the single wire and no wire in between. [Color figure can be viewed in the online issue, which is available at wileyonlinelibrary.com]